

# Molecular Modeling of Conformational Properties of Oligodepsipeptides

Jiajing Zhang, Michael King, Laura Suggs, and Pengyu Ren\*

Department of Biomedical Engineering, University of Texas at Austin, Austin, Texas 78712

Received March 1, 2007; Revised Manuscript Received May 24, 2007

A depsipeptide is a chemical structure consisting of both ester and amide bonds. Quantum mechanics calculations have been performed to investigate the conformational properties of a depsipeptide in the gas and solution phases. Similar to an alanine dipeptide, the depsipeptide exhibits a strong preference for the polyproline II (PPII) helical conformation. Meanwhile, due to the changes in the intramolecular interaction, the propensity for  $\beta$ -sheets and  $\alpha$ -helices diminishes while an unusual inclination for the  $(\phi, \psi) = (-150^\circ, 0^\circ)$  conformation was observed. A molecular mechanics model has been developed for polydepsipeptides based on the quantum mechanical study. Both simulated annealing and replica exchange molecular dynamics simulations have been carried out on oligodepsipeptide sequences with alternating depsi and natural residues in solution. Novel helical structures have been indicated from the simulations. When glycine is used as the alternating natural amino acid residue, the PPII conformation of a depsi residue stabilizes the peptide into a right-handed helical structure while the  $\alpha$ -helical conformation of the depsi residue favors an overall left-handed helical structure. The free energy analysis indicates that both the left- and the right-handed helices are equally likely to exist. When charged lysine is introduced as the alternating natural residue, however, it is found that the depsipeptide sequence prefers an extended conformation as in PPII. Our results indicate that the depsipeptide is potentially useful in designing protein mimetics with controllable structure, function, and chemistry.

## Introduction

There has been a growing interest in engineering novel molecules that can mimic the well-defined structures and diverse functions of naturally occurring proteins and other biomolecules. These mimetics present tremendous opportunities for novel materials and therapeutics.<sup>1,2</sup> Considerable efforts have been made to explore novel peptide-mimetic molecules with specific secondary structures. Examples of interesting peptidomimetics include peptoids,<sup>3–6</sup>  $\beta$ -peptides,<sup>7–12</sup>  $\gamma$ -peptides,<sup>13</sup> and azapeptides,<sup>14,15</sup> which have been shown to fold into stable helices and turns. A common approach to explore novel foldamers is to replace the amide bonds with bioisosteric groups such as carbamate,<sup>16</sup> phosphoramidate,<sup>17,18</sup> and sulfonamide groups.<sup>19–24</sup>

A depsipeptide (“depsi” comes from the Greek word for ester) is a chemical structure consisting of both ester and amide bonds (Figure 1). Even though the structure seems to be “engineered” from amino acids, it actually occurs naturally in certain lactic acid bacteria. Depsipeptides, primarily in cyclic form, have been explored as potential anticancer agents in drug discovery.<sup>25–29</sup> Several research groups have been focusing on the synthesis of polydepsipeptides (PDPs) or polyester amides, consisting of alternating ester and amide functionalities.<sup>30–33</sup> These polymers have potential applications in drug delivery and tissue engineering as they are degradable via hydrolytic scission into biocompatible chemicals.<sup>34</sup> However, no systematic study of PDP secondary structure has been reported due in part to the difficulty of the synthesis and subsequent characterization.

Molecular modeling is becoming a powerful tool for studying molecular behavior at the atomic resolution. Through molecular mechanical calculations, Cohen and co-workers reported that peptoid oligomers containing chiral centers in their side chains present a new structural paradigm. Specifically, it was suggested that an octamer of the S isomer of *N*-(1-phenylethyl)glycine formed a right-handed helix with cis amide bonds.<sup>5</sup> Van

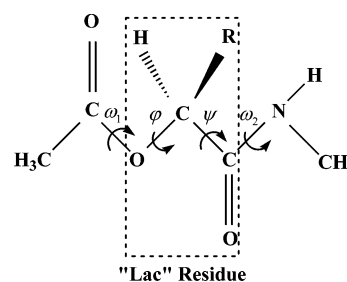


**Figure 1.** Structural formula of the depsi dipeptide studied, with the central residue referred to as a “lac” residue.

Gunsteren and co-workers investigated the stability of helical secondary structures of  $\alpha$ - and  $\beta$ -polypeptides using molecular dynamics (MD) simulations.<sup>10,35,36</sup> Hofmann and co-workers provided a complete overview on helix formation in  $\alpha$ - and  $\beta$ -peptoids via systematic conformation analysis using ab initio molecular orbital theory.<sup>12</sup> Recently, molecular-mechanics-based simulations enjoyed great success in predicting the folding of small proteins.<sup>37,38</sup> Those studies demonstrated that the quantum-mechanics- and molecular-mechanics-based computational approaches are indeed useful in understanding the structure and stability of proteins and protein mimetics and provide insights beyond the reach of current experimental techniques.

In this paper, we report the first attempt to investigate the conformational properties of PDPs and their ability to form stable secondary structures using quantum mechanical calculations and molecular modeling. It is our goal to understand the relationship between the chemistry and conformational propensity of the oligodepsipeptide, which will in turn help us design novel foldamers with various structures and functionalities.

## Computational Details

**Quantum Mechanical Characterization of the Depsidipeptide.** Ab initio quantum mechanical calculations were

\* Author to whom correspondence should be addressed. Phone: (512) 232-1832. Fax: (512)-471-0616. E-mail: pren@mail.utexas.edu.

**Table 1.** OPLSAA/L Atomic Partial Charges for the Natural Residue in Comparison with Partial Charges Derived for Lac

alanine dipeptide $-\text{C}-\text{NH}-\text{C}_\alpha-$ (OPLSAA/L parameters)		lac residue $-\text{C}-\text{O}-\text{C}_\alpha-$ (this work)	
atom	charge ( <i>e</i> )	atom	charge ( <i>e</i> )
N	-0.50	O	-0.32
H	0.30		
C <sub>carbonyl</sub>	0.50	C <sub>carbonyl</sub>	0.65
C <sub>α</sub>	0.14	C <sub>α</sub>	0.11

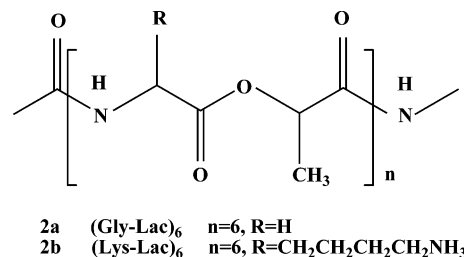
**Table 2.** Parameters for Torsional Potential Term<sup>a</sup>

torsion angle <sup>c</sup>	<i>V</i> <sub>0</sub>	<i>γ</i> <sub>0</sub>	<i>V</i> <sub>1</sub>	<i>γ</i> <sub>1</sub>	<i>V</i> <sub>2</sub>	<i>γ</i> <sub>2</sub>
Ψ <sub>N-Cα-C-O</sub>	0.890 <sup>b</sup>	0.0 <sup>c</sup>	2.180	180.0	-1.090	0.0
Ω <sub>Cα-C-O-Cα</sub>	2.200	0.0	6.330	180.0		
Φ <sub>C-O-Cα-C</sub>	1.852	0.0	0.719	180.0	2.286	0.0
Ψ <sub>O-Cα-C-N</sub>	1.469	0.0	1.853	180.0	-1.382	0.0

<sup>a</sup> The torsional potential is given by  $v(\omega) = \sum_0^N V_n/2[1 + \cos(n\omega - \gamma_n)]$ , where  $\omega$  is the torsion angle. <sup>b</sup> The coefficients are in kcal/mol. <sup>c</sup> The torsion angles are in degrees.

performed on alanine dipeptide and depsipeptide (Figure 1) using the Gaussian 03 package.<sup>39</sup> We refer to the central residue of the depsipeptide in this study as “lac”, in recognition of its conceptual lineage to lactic acid. The conformational energy of the lac and alanine dipeptide with respect to the rotation of the  $\phi$  and  $\psi$  torsion angles was evaluated. Both torsion angles were scanned in increments of 30° from -180° to 180°, resulting in a total of 144 conformers per molecule. Each conformer was optimized using the Gaussian 03 program package<sup>39</sup> with all degrees of freedom relaxed except the torsion angles that were constrained at fixed values. The gas-phase energy of each conformer was then evaluated at the MP2/6-311++G(2d,2p) level. The solvation energy in water was estimated with the implicit polarizable continuum model.<sup>40</sup> An OPLSAA/L-type<sup>41,42</sup> molecular mechanics model was developed for the depsipeptide based on the ab initio study. The partial charges for new atom types in the lac residue were derived at the MP2/6-31G\* level to be consistent with OPLSAA parameters. The atomic partial charges for the lac residue were derived by fitting to the electrostatic potential (ESP).<sup>43</sup> To obtain a set of charges consistent with those used by OPLSAA, we have fixed the charges of all atoms, except those of the ester oxygen, directly bonded atoms to the carbonyl carbon and C<sub>α</sub>, at original OPLSAA values for peptides in the ESP fit. Essentially, we only allow the partial charges for the above three atoms to change. The missing torsional parameters were obtained by comparison with ab initio conformational energies. The OPLSAA/L partial charges and torsional parameters for lac were summarized in Tables 1 and 2. The van der Waals parameters ( $3.0000 \times 10^{-1}$  and  $7.1128 \times 10^{-1}$ ) for ester O were transferred from the OPLSAA ester group. For any other parameters that are not listed, OPLSAA values have been used.

**Molecular Dynamics Simulations.** All of the MD simulations, including simulated annealing, were performed on the 12-residue depsipeptide sequences with alternating lac and natural residues (Figure 2) in a box of explicit water molecules. Both peptides were terminated with acetyl and *N*-methyl groups at the N and C termini, respectively. In this study we chose glycine or lysine as the natural residues for the contrast in size, charge, and hydrophobicity. Molecular dynamics simulations with explicit solvent (water) were carried out using the GROMACS program package. We used the OPLSAA/L force field<sup>44,45</sup> for glycine/lysine and Cl<sup>-</sup> and the SPC model<sup>46</sup> for water. For the depsipeptide, we derived parameters compatible with OPLSAA/L as described above. The depsipeptides were soaked in a periodic cubic box of water molecules, with 30 Å on a side

**Figure 2.** Chemical formula of the polydepsipeptide studied. (a) R stands for H and *n* = 6 for 12 alternating glycine and lac residues, which was referred to as “Gly-lac”. (b) R = CH<sub>2</sub>CH<sub>2</sub>CH<sub>2</sub>CH<sub>2</sub>NH<sub>3</sub><sup>+</sup> and *n* = 6 for 12 alternating lysine and lac residues, which was referred to as “Lys-lac”.

for the Gly-lac and 40 Å for the Lys-lac system. Counterions were also introduced in Lys-lac in replica exchange molecular dynamics (REMD) as described later. The cell dimension was selected to ensure that the separation between the peptide and its own image would be at least 15 Å. The greater size was needed for Lys-lac due to its bulkier side chain. All of the bond lengths were constrained using the LINCS algorithm,<sup>47</sup> and the default values for the LINCS parameters in GROMACS were used. The temperature was controlled using the Nosé-Hoover thermostat.<sup>48,49</sup> The long-range electrostatic interactions were treated with particle-mesh Ewald summation<sup>50,51</sup> with a real space cutoff of 9 Å. A time step of 2 fs was used in all MD simulations.

Simulated annealing, a global minimization algorithm, was utilized to search for stable structures. High temperature allows the molecule to explore conformational space much more efficiently. Three independent simulated annealing runs were performed for Gly-lac and Lys-lac. In each run, the system temperature was first heated from 300 up to 1000 K in 0.5 ns, and then it was gradually cooled down to absolute zero by the default linear cooling schedule in 30 ns for Gly-lac and 40 ns for Lys-lac (without counterions). The longer annealing time was used for Lys-lac due to its greater degrees of freedom. After annealing, two stable Gly-lac structures and one Lys-lac structure were subject to an additional 30 ns of canonical (NVT) MD simulations at room temperature to sample the peptide conformational space, from which the conformational free energy maps in the ( $\phi, \psi$ ) dimensions were constructed for each type of residue.

**Replica Exchange Molecular Dynamics Simulation.** Due to the large number of degrees of freedom in the 12-mer peptides, there exists a large number of energy minima separated by high-energy barriers (compared to thermal motion). As a result, simulated annealing is not guaranteed to locate the global minimum. The REMD method is particularly useful for exploring the conformational space of peptides and small proteins.<sup>52–54</sup> The REMD algorithm can be summarized as follows: (i) Several replicas (*i* = 1, 2, ..., *N*) are simulated at fixed temperatures *T<sub>n</sub>* (*n* = 1, 2, ..., *N*) simultaneously and independently for a certain number of Monte Carlo or MD steps. (ii) A pair of replicas at neighboring temperatures is selected, and the exchange is attempted with the acceptance ratio

$$w(X \rightarrow X') = w(x_n^{[i]} | x_{n+1}^{[j]}) = \begin{cases} 1, & \Delta \leq 0 \\ \exp(-\Delta), & \Delta > 0 \end{cases} \quad (1)$$

where  $\Delta = [\beta_n - \beta_{n+1}](E(q^{[i]}) - E(q^{[j]}))$ . Here  $\beta_n$  and  $\beta_{n+1}$  are two reciprocal temperatures,  $q^{[i]}$  is the configuration at  $\beta_n$ ,  $q^{[j]}$  is the configuration at  $\beta_{n+1}$ , and  $E(q^{[i]})$  and  $E(q^{[j]})$  are potential energies of the systems at these two configurations, respectively.

As a result, REMD allows the search for conformational space accessible at high temperatures. In this study, two sets of REMD simulations were performed on the Lys-lac systems with and

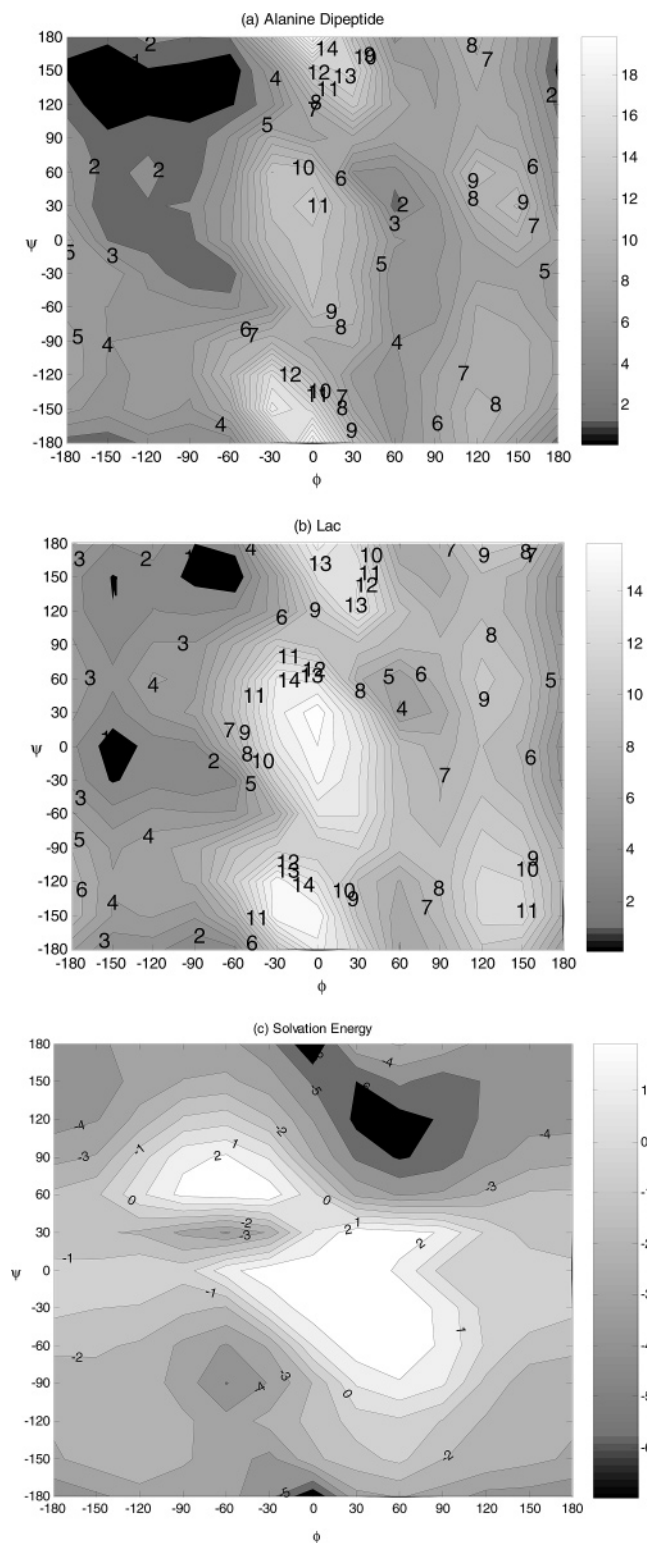


**Figure 3.** (a) Quantum mechanical conformational free energy contour map of alanine dipeptide in solution, (b) quantum mechanical conformational free energy map of depsi dipeptide, and (c) the corresponding solvation energy contribution from polarizable continuum model. All of the free energies are in the units of kcal/mol.

without neutralizing counterions. In the first set of REMD, the 12-residue sequence with alternating lysine and lac was placed in a periodic cubic box containing 2340 water molecules and no counterion, with 40 Å on each side. In the other set of REMD, 6 Cl<sup>−</sup> counterions and 3194 water molecules were used in a cubic box with 46 Å on each side, resulting in a total salt concentration of 0.10 M. To ensure that the temperatures were

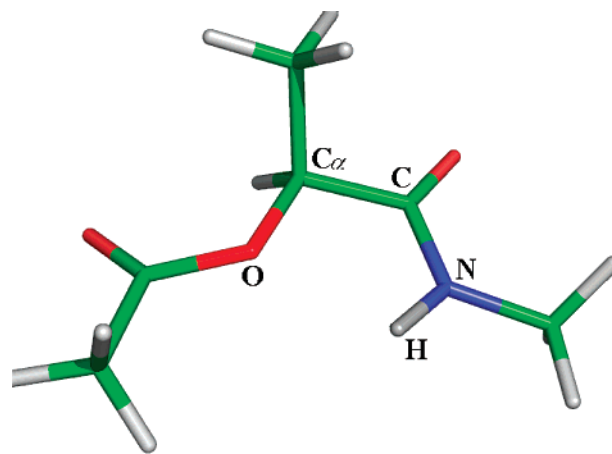


**Figure 4.** Intramolecular interactions that stabilize the (−150°,0°) conformation of the depsipeptide.

optimally distributed and the number of replicas was sufficient, different temperature gaps from 2.6 to 7.6 K were used between the neighboring replicas. These gaps were chosen to maintain the success rates of exchange between replicas within 36–44%. With the temperature ranging from 282.5 to 602.3 K, we simulated a total of 73 replicas of Lys–lac in solution. To generate a set of initial configurations that broadly covers the conformational space of the depsipeptide, we chose 73 starting configurations randomly from the annealing MD simulation trajectory. Each replica was subject to 6.0 ns of MD simulation with a time step of 2 fs, with configurations saved every 2 ps. The exchanges were attempted every 0.4 ps, with the acceptance ratio determined by the Metropolis criterion, which is shown in eq 1.

**Free Energy Map.** The free energy map was obtained by calculating the probability  $P(x,y)$  from a histogram analysis of the room-temperature MD simulation.<sup>54–56</sup>

$$P(x,y) = \frac{1}{Z} \exp[-\beta W(x,y)] \quad (2)$$

where  $(x,y)$  is any specified set of reaction coordinates, i.e.,  $(\phi,\psi)$ .  $P(x,y)$  is the frequency of the molecule appearing and observed at  $(x,y)$  during the simulation, and  $Z$  is the configurational partition function. The relative free energy difference between two reaction coordinates can be expressed as

$$F(x,y) = W(x_2,y_2) - W(x_1,y_1) = -RT \log \left[ \frac{P(x_2,y_2)}{P(x_1,y_1)} \right] \quad (3)$$

We first calculated and collected all the backbone  $(\phi,\psi)$  torsion angles for each type of residue from the MD trajectory. A two-dimensional histogram of the torsional angle distribution was constructed using 144 bins between  $-180^\circ$  and  $+180^\circ$  in both  $\phi$  and  $\psi$  dimensions. The probability of a given  $(\phi,\psi)$  was then calculated by normalizing the population in each bin. The lowest free energy in the map was set to be zero.

Following the work of Pappu and co-workers,<sup>57</sup> we also explored the free energy landscape using the asphericity  $\langle\delta\rangle$  and the radius of gyration  $\langle R_g\rangle$  as two reaction coordinates. For a given peptide conformer, the instantaneous asphericity is defined as

$$\delta = 1 - 3 \frac{l_1^2 l_2^2 + l_2^2 l_3^2 + l_3^2 l_1^2}{(l_1^2 + l_2^2 + l_3^2)^2} \quad (4)$$



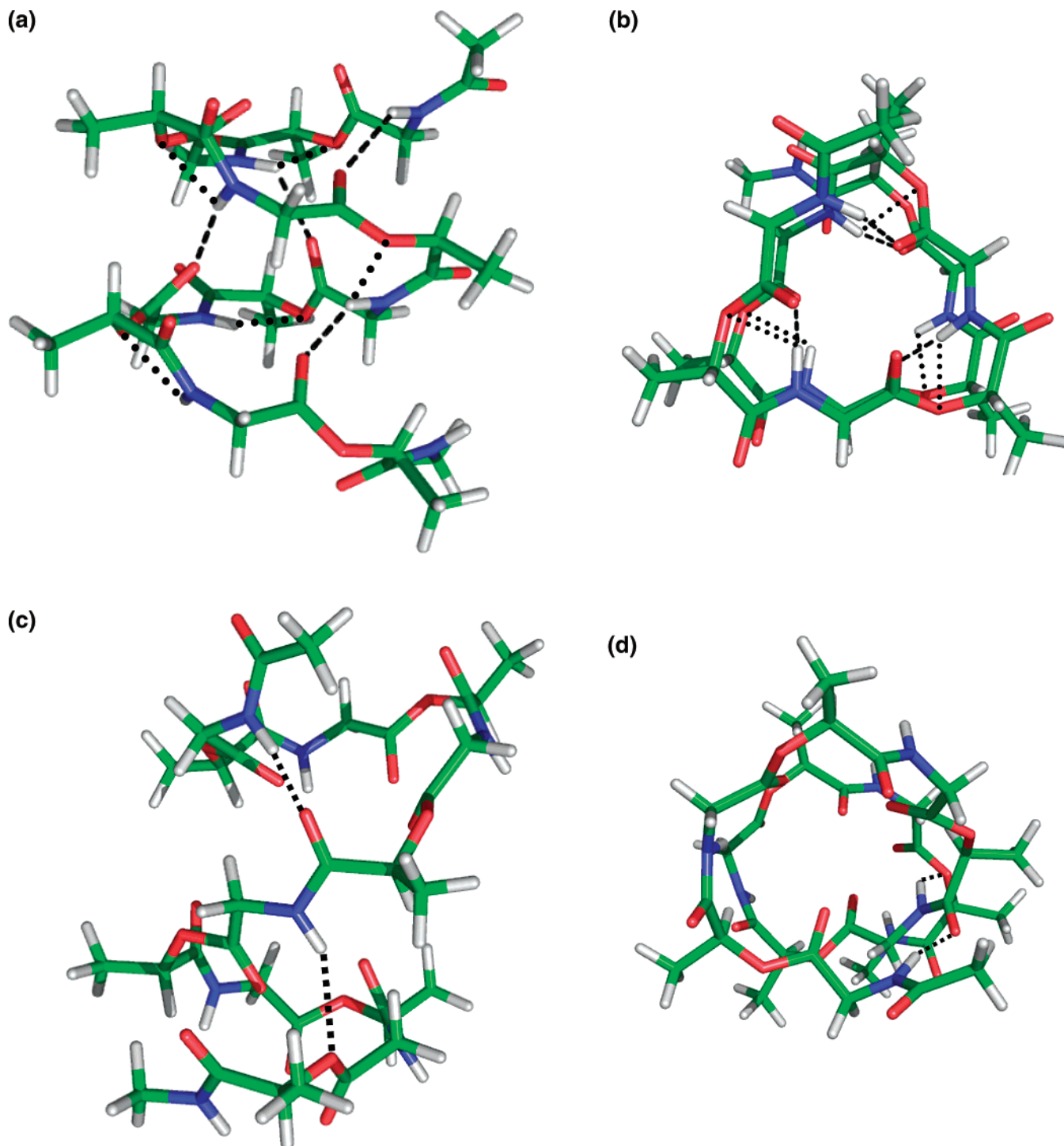


**Figure 5.** Typical interactions in the Gly-lac depsipeptide for the (a and b) left- and (c and d) right-handed helix. Parts a and c illustrate the helices looking down the long axis, and parts b and d show the side views of the two helices, respectively. The carbon atoms are shown in green, nitrogen in blue, oxygen in red, and hydrogen in white. Note that the dotted lines indicate the “1–5 intra” interactions between the deprotonated oxygen ( $i$ ) and NH ( $i + 1$ ) ( $i = 2, 4, 6, 8, 10$ ), and the interactions between NH ( $i$ ) and CO ( $i + 4$ ) ( $i = 1, 3, 5, 7$ ) were represented by the dashed lines.

where  $l_1$ ,  $l_2$ , and  $l_3$  are eigenvalues of the instantaneous gyration tensor  $T$ .<sup>69</sup> And the instantaneous radius of gyration  $R_g$  is determined by  $R_g = \sqrt{\text{Trace}(T)}$ , where  $\text{Trace}(T)$  is the trace of the instantaneous gyration tensor. Asphericity quantifies the shape of any arbitrary peptide; it becomes 1 for a rodlike shape and 0 for a perfect sphere. The radius of gyration describes the average size of a molecule.

For REMD, the weighted histogram analysis method that combines data from all temperature replicas (T-WHAM) was used to obtain the room-temperature potential of mean force of

the residues with respect to torsion angles.<sup>58</sup> This method improves the sampling in the high-energy regions at room temperature. Data from two sets of REMD simulations, without and with counterions, were utilized to construct the potential of mean force of Lys and lac residues with respect to  $\phi$  and  $\psi$ .

In summary, ab initio quantum mechanical calculations were first performed to obtain charges and torsional parameters and to characterize conformational properties of the solvated dipeptides. All of the following simulations were carried out within the framework of molecular mechanics and molecular dynamics.

Simulated annealing runs for Gly–lac and Lys–lac were performed to find the most stable structures. Starting from those structures, room-temperature MD runs were carried out to sample the peptide conformational space, from which the free energy surface maps in the  $(\phi, \psi)$  and  $(R_g, \delta)$  dimensions were constructed. We further utilized REMD simulations for the Lys–lac peptide to fully sample the configurational space and investigate the effects of counterions, from which conformational free energy maps were obtained and compared with those from room-temperature MD runs.

## Results and Discussion

**Ab Initio Characterization of Conformational Properties of the Depsipeptide.** We have investigated conformational energy of both depsi (Figure 1) and alanine dipeptides. The only difference between the two chemical structures is that the amide NH group in alanine is replaced by oxygen in the depsidi peptide. As shown in Table 1, changing from the alanine to depsi dipeptide, the atomic charges were redistributed around the depsi group as the oxygen atom is slightly more electronegative than the NH.

Following the classic approach to the Ramachandran plot,<sup>59</sup> we calculated the relative free energies with respect to the backbone conformation for both the depsi and the alanine dipeptide in solution (Figures 3a and 3b) based on quantum mechanical calculations. The solvation energy contribution for lac computed from the polarizable continuum model was also illustrated in Figure 3c. We have further compared our results on alanine dipeptide with a previous study where the whole system (alanine and solvent) is treated with quantum mechanics.<sup>60</sup> In agreement with our results, the polyproline II (PPII) conformation was identified as the global minimum on the potential energy surface. Similar to an alanine dipeptide, the “lac” residue exhibits a strong preference for the PPII helical conformation as well. In addition, an unusual inclination for the  $(-150^\circ, 0^\circ)$  conformation was observed. While the substitution of the oxygen atoms eliminates the ability to form hydrogen bonds between peptide bonds, the “1–5” intrasidue interaction shown in Figure 4 seems to have stabilized this conformation. Also note that this interaction would lock the  $\psi$  angle near  $0^\circ$  but has little influence on the rotation of the  $\phi$  angle.

**Global Search for the Stable Structures.** To examine the effect of the side chain chemistry on the depsipeptide conformation, two depsipeptide sequences with alternating lac and natural residues, either glycine or lysine, were investigated (Figure 2). While glycine is nonpolar and has no side chain, lysine is a charged, hydrophilic residue with a bulky side chain. Glycine occurs frequently in the turn regions of proteins where other residues would be sterically hindered. Three independent simulated annealing runs were applied to search for stable structures for Gly–lac and Lys–lac (without counterions).

For the Gly–lac alternating sequence, two simulated annealing runs showed that the depsipeptide folded into well-defined, noncanonical helical secondary structures at 298 K, one left-handed and the other right-handed (Figure 5). During the third annealing run, the peptide switched back and forth between the two and displayed a mixed structure at the end of annealing.

In the Lys–lac case, a PPII-like extended left-handed helical structure was obtained from all three runs as the minimum-energy conformation. An example structure is illustrated in Figure 6.

**MD/REMD Simulation and Free Energy Landscape.** Three NVT molecular dynamics simulations starting from the

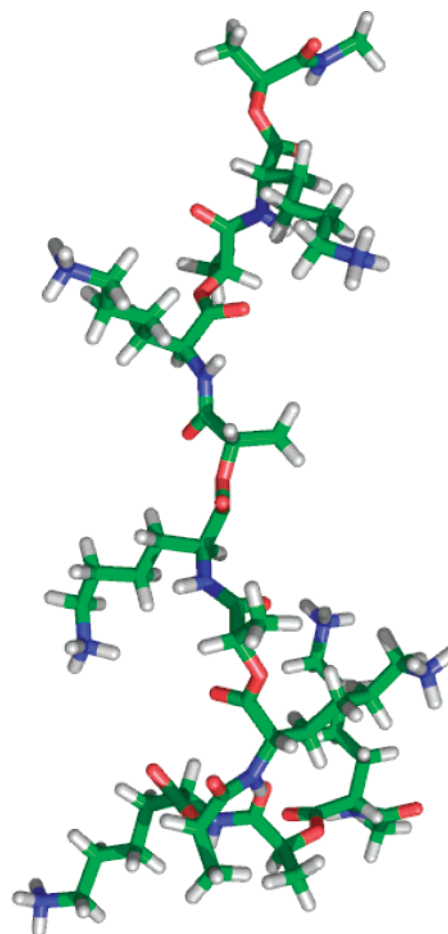


**Figure 6.** Typical PPII-like structure of the Lys–lac depsipeptide. This structure was obtained from simulated annealing without counterions. The carbon atoms are shown in green, nitrogen in blue, oxygen in red, and hydrogen in white.

above stable conformers, left- and right-handed Gly–lac helices and extended Lys–lac (without counterions), were performed at 298 K, from which the conformational free energy maps were calculated for each type of residue.

The left- and right-handed helices of Gly–lac were well-maintained during the room-temperature MD simulation, with the structure partially unfolded to PPII-like structure or irregular turns only occasionally. No significant difference in the conformational population was observed between the left-handed and the right-handed helix simulation trajectories for both the glycine and the lac residues. The results of the two were thus combined, and the corresponding free energy contour maps are shown in Figure 8. The glycine residue undertakes  $\phi$  and  $\psi$  angles in all four quadrants of the map as expected due to the lack of chirality. In comparison to the glycine Ramachandran plot analyzed from the Protein Data Bank,<sup>61</sup> the population in the helical region predicted by OPLSAA/L is relatively low in Figure 8; for the lac residue, the local and global minima reside inside  $(-90^\circ$  to  $-60^\circ, -30^\circ)$  and  $(-90^\circ$  to  $-60^\circ, +150^\circ)$ , which approximately corresponds to right-handed  $\alpha$ - and PPII-helical conformations.

However, the lac residue in the Lys–lac room-temperature MD simulation showed little sampling at the  $(-150^\circ, 0^\circ)$  conformation (Figure 9b). Although there is still a slight possibility to adopt the  $\alpha$ -helical structure, the minimum-energy conformation is predominantly PPII-like, corresponding to the  $(-90^\circ, 150^\circ)$  region. For the lysine residue, the preferred conformation is limited to a similar range of dihedral angles

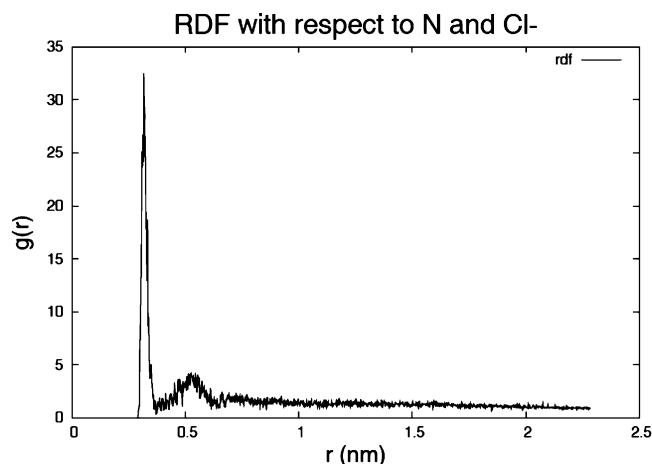


**Figure 7.** Radial distribution function with respect to  $\text{Cl}^-$  ions and terminal N atoms in lysine residues. The distance is given in nanometers.

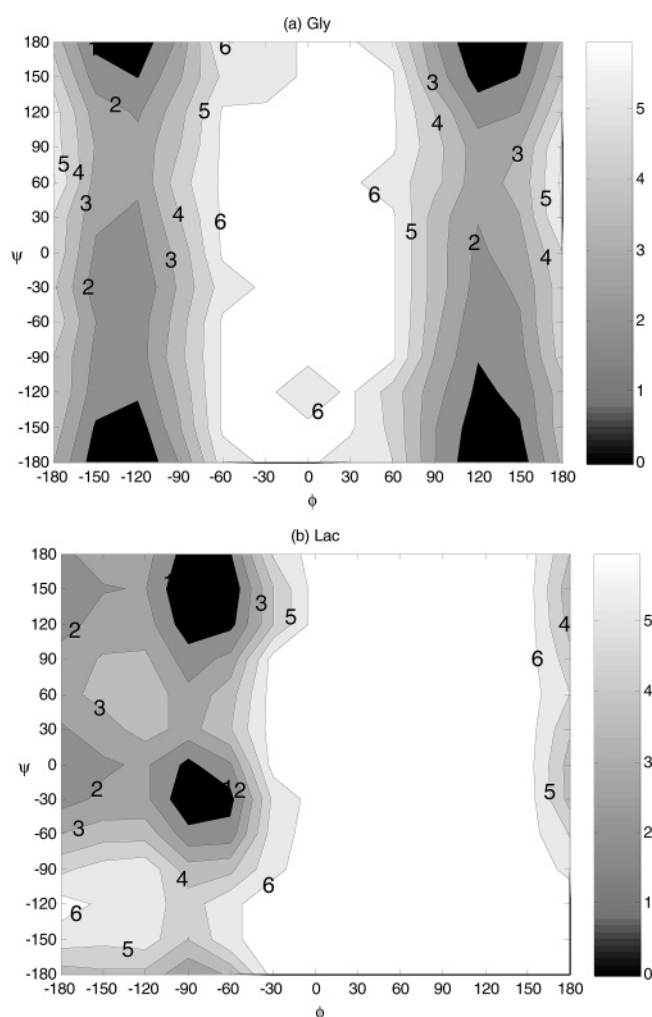


**Figure 8.** Conformational free energy contour maps for (a) the glycine and (b) lac residues in Gly-lac. Maps are plotted based on the data from room-temperature MD runs.

( $-90^\circ$  to  $-60^\circ$ ,  $150^\circ$ ). As a result, the Lys-lac peptide exists mostly in the PPII-like extended conformation.

The effect of counterions on the charged peptide conformation was also considered. In a previous study of the effect of ionic strength on free energy calculations, Donnini et al. concluded that it is best to include no ions or a high concentration of counterions due to sampling issues.<sup>62</sup> As suggested, two sets of

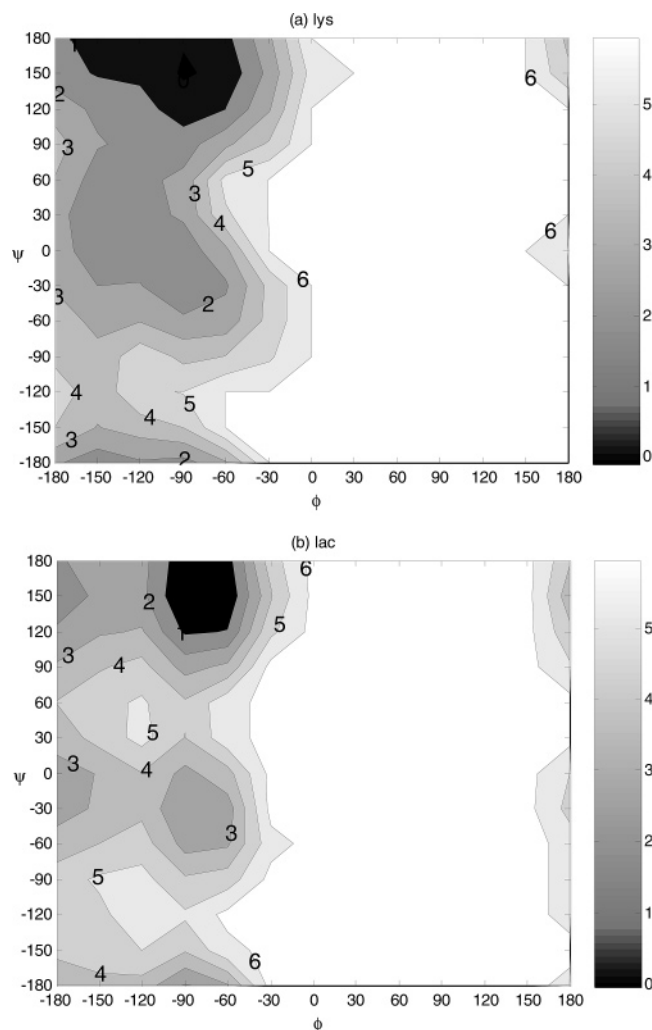


**Figure 9.** Conformational free energy contour maps for (a) the lysine and (b) lac residues in Lys-lac. Maps are plotted based on the data from room-temperature MD runs.

the REMD simulations were performed, where one has six neutralizing  $\text{Cl}^-$  ions and the other has no counterions. We have further calculated the conformational free energy of Lys-lac from the REMD simulation using T-WHAM. The resulting free energy maps are compared in Figure 10. Overall the free energy maps obtained from the room-temperature MD (Figure 9) and REMD are in very good agreement for Lys-lac without counterions. Both methods have identified that the global energy minima of the lysine and lac residues reside in the same PPII regions. However, the room-temperature MD clearly has much less population in the high-energy region as expected. In contrast, REMD samples a much broader configurational space. We further examined the convergence to ensure sufficient sampling of the ions for the simulations with counterions. The radial distribution function (RDF) with respect to  $\text{Cl}^-$  ions and terminal N atoms in lysine residues is plotted in Figure 7. The sharp peak at  $d = 0.31$  nm in the RDF plot reveals the strong interaction between terminal N atoms and counterions.

REMD data from the simulation without (Figures 10a and 10b) and with 6 counterions (Figures 10c and 10d) were also compared. Given there are 6 ions and 6 charged N-termini, the RDF that we obtained, and the help of high-temperature sampling provided by REMD, we believe that the sampling is converged. However, the results, with or without counterions, are very similar, within the statistical uncertainties of our simulation.



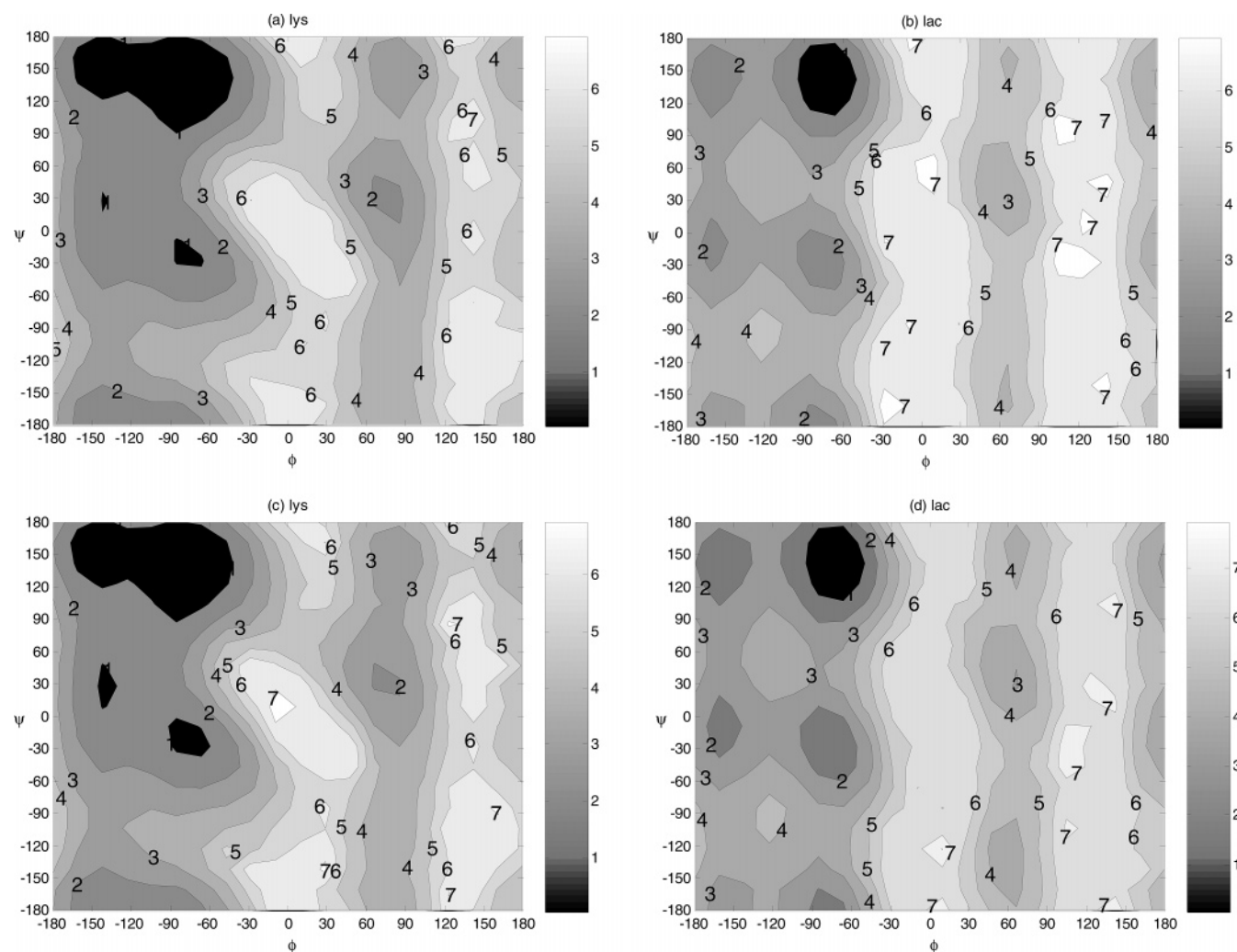


**Figure 10.** Conformational free energy maps of the Lys and lac residues. The free energies were calculated from 73 REMD simulations using T-WHAM: (a) Lys without counterions; (b) lac without counterions; (c) Lys with counterions; (d) lac with counterions.

The free energy landscape characterized by the asphericity ( $\delta$ ) and the radius of gyration ( $R_g$ ) were also constructed for the Gly-lac and Lys-lac peptides in Figures 11a and 11b, respectively. As the radius of gyration ( $R_g$ ) is an indicator of the overall size and asphericity ( $\delta$ ) quantifies the shape of the peptide, we can roughly distinguish between the left- and the right-handed helical structures using these two degrees of freedom. For the Gly-lac sequence, the right-handed helical structure typically resides in the ( $R_g = 0.55$  nm,  $\delta = 0.35-0.55$ ) area while the left-handed helical structure is roughly near ( $R_g = 0.5-0.55$  nm,  $\delta = 0.1-0.2$ ). For the Lys-lac sequence, however, the asphericity value is almost 1, consistent with the observation of a more extended structure.

**Structure Characterization.** Table 3 lists the typical torsion angles found in the left- and right-handed helices of Gly-lac (corresponding to Figure 5). It is noted that glycine can adopt a conformation in any of the quadrants in the free energy map. However, when the glycine undertakes a conformation in the bottom-left quadrant ( $-120^\circ, -160^\circ$ ), the  $\alpha$ -helical conformation of lac facilitates the adoption of the left-handed helix structure by the 12-mer. Meanwhile, the combination of glycine in the bottom-right quadrant and lac in the PPII-helical conformation favors the right-handed helical structure sterically.

In the left-handed helix, the helical turns are characterized by the “1–5 intra” interaction between the lac oxygen ( $i$ ) and Gly NH ( $i + 1$ ) ( $i = 2, 4, 6, 8, 10$ ) discussed above. The adjacent turns are stabilized by the interaction between at NH ( $i$ ) and

CO ( $i + 4$ ) ( $i = 1, 3, 5, 7$ ). This kind of left-handed helix is found to possess 6 residues per turn and gives an average rise per residue of about 8 Å. In the right-handed helical structure, however, there seems to be no well-defined hydrogen-bonding pattern or interaction. The right-handed helix holds approximately 6 residues per turn and an average rise per residue of about 9 Å.

It is in general difficult for short peptides to sustain stable secondary structures without the assistance of other factors such as tertiary contact. In reality, they likely exist in an ensemble of stable structures and interconvert between them over time. With detailed MD simulation, we have the opportunity to address questions such as what fraction of the Gly-lac decapeptide exists in a folded conformation and how often it forms the left-handed versus the right-handed helical structure. To address the first question, we can assess the population of well-defined structures directly from the free energy map that we have obtained. On the basis of Figure 11a, the right-handed helical structure typically resides in the ( $R_g = 0.55$  nm,  $\delta = 0.35-0.55$ ) area while the left-handed helical structure is near ( $R_g = 0.50-0.55$  nm,  $\delta = 0.10-0.20$ ). Even though it is difficult to draw conclusions on the relative stability of left-handed versus right-handed helices, the two areas combined account for over 60% of total population. The remaining shallow area represents random structures, which may consist of both left- and right-handed helical motifs in one structure. We have further traced both of the left- and right-handed helical conformers in the  $\phi$ - $\psi$

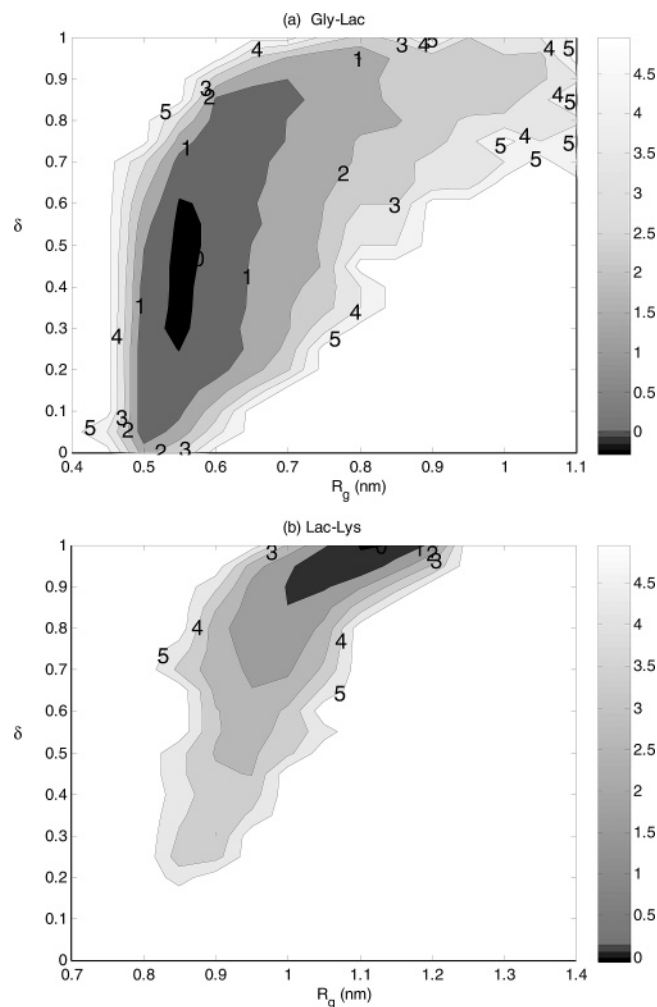


**Figure 11.** (a) Free energy contour map of Gly-lac shown using  $\delta$  and  $R_g$  as two reaction coordinates. Note that the map was derived by combining the two room-temperature MD runs starting with right- and left-handed helical structures. (b) Free energy contour map of the Lys-lac peptide with respect to  $\delta$  and  $R_g$ . This map was derived from the room-temperature MD simulation of Lys-lac.

**Table 3.** Typical Geometry Data for Gly and Lac Residues from Left- and Right-Handed Helical Structures<sup>a</sup>

$\Phi_{\text{Gly}}$	$\Psi_{\text{Gly}}$	$\Phi_{\text{Lac}}$	$\Psi_{\text{Lac}}$
Torsion Angles in Left-Handed Helix			
-119.76	-162.15	-79.29	-0.87
-106.16	-158.93	-70.76	-20.57
-118.58	-158.27	-82.10	-2.70
-122.17	-150.71	-74.55	-11.41
-120.87	-149.51	-76.07	-13.69
Torsion Angles in Right-Handed Helix			
125.92	-154.10	-69.55	128.21
123.46	160.91	-70.71	120.80
140.62	-176.07	-78.33	146.71
121.76	-132.12	-70.83	130.88
112.70	-161.19	-77.79	134.82

<sup>a</sup> All of the torsion angles are in degrees.

energy map of the lac residue (Figure 8b) as the two dominant minima of lac, PPII and  $\alpha$ -helix, are responsible for right- and left-handed helices, respectively. Although the PPII region is the global minimum area, the population is only slightly higher than that of the  $\alpha$  helix region. Thus, given the statistical uncertainty in our sampling and accuracy in the force field potential, we conclude that there is roughly an equal probability

for the Gly-lac sequence to adopt either the left- or the right-handed helical conformation.

The Lys-lac peptide exists mostly as an extended left-handed helix, as shown in Figure 6. PPII lacks intramolecular hydrogen bonds but is more exposed to solvent. It has been suggested that the main chain tends to have a regular pattern of hydrogen bonds with water and the main chain-water hydrogen bonding is the major stabilizing factor.<sup>63</sup> For Lys-lac, the intramolecular interaction is rather different from that in the natural peptides due to the replacement of the NH group by an oxygen atom; thus the ability of forming canonical  $\beta$ -sheets or  $\alpha$ -helices diminishes. In addition, it is reported that charged lysine residues favor PPII structure because of the electrostatic repulsion between the side chains and better solvation when extended.<sup>64–68</sup> It is known that solution conditions such as salt concentration have a strong influence on peptide structures. Our REMD study however indicates that Lys-lac prefers the extended PPII-like conformation with or without neutralizing counterions. Further study considering salt effects, ionic strength, pH value, and temperature is necessary to fully understand the conformational properties of peptides containing charged lysine.

## Conclusion

Quantum-mechanics- and molecular-mechanics-based calculations and simulations have been performed to investigate the conformational properties of oligodepsipeptides. Quantum mechanics calculations on the lac dipeptide reveal an unusual conformational minimum due to 1–5 intramolecular interactions between the depsi oxygen and the amide hydrogen. The global minimum-energy conformation of depsipeptide is, however, PPII-like, similar to that of the alanine dipeptide.

A molecular mechanics model has been subsequently established and utilized in the simulated annealing and MD simulations of oligodepsipeptides in solution. The MD simulation results indicate that oligodepsipeptides are capable of forming stable, novel secondary structures that are associated with atypical intramolecular interaction. A 12-residue depsipeptide of alternating lac and glycine may adopt either a left- or a right-handed structure with roughly equal opportunities. It is determined that the PPII-helical conformation of lac stabilizes the 12-mer peptide into a right-handed helix while the  $\alpha$ -helical conformation of lac plays a key role in the left-handed helical structure. When the charged lysine is used as the alternating residue, the depsipeptide displays a strong preference for extended left-handed helical polyproline II structure. Our results demonstrate that there is a great potential to achieve novel secondary structures with a depsipeptide of controlled chemistry and sequences.

**Acknowledgment.** Acknowledgment is made to the donors of the American Chemical Society Petroleum Research Fund for supporting this research. The authors also thank the Texas Advanced Computing Center (<http://www.tacc.utexas.edu>) at The University of Texas at Austin for providing high-performance computing resources that have contributed to the research results reported within this paper.

## References and Notes

- Zhang, S. G.; Marini, D. M.; Hwang, W.; Santoso, S. Design of nanostructured biological materials through self-assembly of peptides and proteins. *Curr. Opin. Chem. Biol.* **2002**, 6 (6), 865–871.
- Kee, S.; Jois, S. D. S. Design of  $\beta$ -turn based therapeutic agents. *Curr. Pharm. Des.* **2003**, 9 (15), 1209–1224.



- (3) Simon, R. J.; Kania, R. S.; Zuckermann, R. N.; Huebner, V. D.; Jewell, D. A.; Banville, S.; Ng, S.; Wang, L.; Rosenberg, S.; Marlowe, C. K.; Spellmeyer, D. C.; Tan, R. Y.; Frankel, A. D.; Santi, D. V.; Cohen, F. E.; Bartlett, P. A. Peptoids—A modular approach to drug discovery. *Proc. Natl. Acad. Sci. U.S.A.* **1992**, *89* (20), 9367–9371.
- (4) Mohle, K.; Hofmann, K. J. Secondary structure formation in N-substituted peptides. *J. Pept. Res.* **1998**, *51* (1), 19–28.
- (5) Armand, P.; Kirshenbaum, K.; Falicov, A.; Dunbrack, R. L.; Dill, K. A.; Zuckermann, R. N.; Cohen, F. E. Chiral N-substituted glycines can form stable helical conformations. *Folding Des.* **1997**, *2* (6), 369–375.
- (6) Armand, P.; Kirshenbaum, K.; Goldsmith, R. A.; Farr-Jones, S.; Barron, A. E.; Truong, K. T. V.; Dill, K. A.; Mierke, D. F.; Cohen, F. E.; Zuckermann, R. N.; Bradley, E. K. NMR determination of the major solution conformation of a peptoid pentamer with chiral side chains. *Proc. Natl. Acad. Sci. U.S.A.* **1998**, *95* (8), 4309–4314.
- (7) Iverson, B. L. Chemical synthesis—Betas are brought into the fold. *Nature* **1997**, *385* (6612), 113–115.
- (8) Seebach, D.; Matthews, J. L.  $\beta$ -Peptides: A surprise at every turn. *Chem. Commun.* **1997**, (21), 2015–2022.
- (9) Gellman, S. H. Foldamers: A manifesto. *Acc. Chem. Res.* **1998**, *31* (4), 173–180.
- (10) Soares, T.; Christen, M.; Hu, K. F.; van Gunsteren, W. F. Alpha- and beta-polypeptides show a different stability of helical secondary structure. *Tetrahedron* **2004**, *60* (35), 7775–7780.
- (11) Mohle, K.; Gunther, R.; Thormann, M.; Sewald, N.; Hofmann, H. J. Basic conformers in  $\beta$ -peptides. *Biopolymers* **1999**, *50* (2), 167–184.
- (12) Baldauf, C.; Gunther, R.; Hofmann, H. J. Helices in peptoids of  $\alpha$ - and  $\beta$ -peptides. *Phys. Biol.* **2006**, *3* (1), S1–S9.
- (13) Hanessian, S.; Luo, X. H.; Schaum, R.; Michnick, S. Design of secondary structures in unnatural peptides: Stable helical  $\gamma$ -tetra-, hexa-, and octapeptides and consequences of  $\alpha$ -substitution. *J. Am. Chem. Soc.* **1998**, *120* (33), 8569–8570.
- (14) Han, H.; Yoon, J.; Janda, K. D. Investigations of azapeptides as mimetics of Leu-enkephalin. *Bioorg. Med. Chem. Lett.* **1998**, *8* (1), 117–120.
- (15) Thormann, M.; Hofmann, H. J. Conformational properties of azapeptides. *J. Mol. Struct.: THEOCHEM* **1999**, *469*, 63–76.
- (16) Cho, C. Y.; Moran, E. J.; Cherry, S. R.; Stephans, J. C.; Fodor, S. P. A.; Adams, C. L.; Sundaram, A.; Jacobs, J. W.; Schultz, P. G. An unnatural biopolymer. *Science* **1993**, *261* (5126), 1303–1305.
- (17) Rushing, S. D.; Hammer, R. P. Synthesis of phosphonamide and thiophosphonamide dipeptides. *J. Am. Chem. Soc.* **2001**, *123* (20), 4861–4862.
- (18) Sawa, M.; Kiyoi, T.; Kurokawa, K.; Kumihara, H.; Yamamoto, M.; Miyasaka, T.; Ito, Y.; Hirayama, R.; Inoue, T.; Kirii, Y.; Nishiwaki, E.; Ohmoto, H.; Maeda, Y.; Ishibushi, E.; Inoue, Y.; Yoshino, K.; Kondo, H. New type of metalloproteinase inhibitor: Design and synthesis of new phosphonamide-based hydroxamic acids. *J. Med. Chem.* **2002**, *45* (4), 919–929.
- (19) Calcagni, A.; Gavuzzo, E.; Lucente, G.; Mazza, F.; Pinnen, F.; Pochetti, G.; Rossi, D. Structure and conformation of peptides containing the sulfonamide junction. 3. Synthesis, crystal and molecular structure of a taurine containing peptide oxa-cycle. *Int. J. Pept. Protein Res.* **1991**, *37* (3), 167–173.
- (20) Luisi, G.; Calcagni, A.; Pinnen, F.  $\psi(\text{SO}_2\text{-NH})$  Transition-state isosteres of peptides—Synthesis of the glutathione disulfide analog [Glu- $\psi(\text{SO}_2\text{-NH})$ -Cys-Gly]<sub>2</sub>. *Tetrahedron Lett.* **1993**, *34* (14), 2391–2392.
- (21) Calcagni, A.; Rossi, D.; Paradisi, M. P.; Lucente, G.; Luisi, G.; Gavuzzo, E.; Mazza, F.; Pochetti, G.; Paci, M. Peptides containing the sulfonamide junction: Synthesis, structure, and conformation of Z-Tau-Pro-Phe-NHPr. *Biopolymers* **1997**, *41* (5), 555–567.
- (22) Calcagni, A.; Gavuzzo, E.; Lucente, G.; Mazza, F.; Morera, E.; Paradisi, M. P.; Rossi, D. Peptides containing the sulfonamide junction. 2. Structure and conformation of Z-Tau-Pro-D-Phe-NHPr. *Biopolymers* **2000**, *54* (6), 379–387.
- (23) Moree, W. J.; Vandermarel, G. A.; Liskamp, R. J. Synthesis of peptidosulfonamides and peptidosulfonamides: peptidomimetics containing the sulfonamide or sulfonamide transition-state isostere. *J. Org. Chem.* **1995**, *60*, (16), 5157–5169.
- (24) Baldauf, C.; Günther, R.; Hofmann, H.-J. Conformational properties of sulfonamido peptides. *J. Mol. Struct.: THEOCHEM* **2004**, *675* (1–3), 19–28.
- (25) Li, K. W.; Wu, J.; Xing, W. N.; Simon, J. A. Total synthesis of the antitumor depsipeptide FR-901,228. *J. Am. Chem. Soc.* **1996**, *118* (30), 7237–7238.
- (26) Konstantinopoulos, P. A.; Vondoros, G. P.; Papavassiliou, A. G. FK228 (depsipeptide): A HDAC inhibitor with pleiotropic antitumor activities. *Cancer Chemother. Pharmacol.* **2006**, *58* (5), 711–715.
- (27) Nguyen, D. M.; Schrupp, W. D.; Tsai, W. S.; Chen, A.; Stewart, J. H.; Steiner, F.; Schrupp, D. S. Enhancement of depsipeptide-mediated apoptosis of lung or esophageal cancer cells by flavopiridol: Activation of the mitochondria-dependent death-signaling pathway. *J. Thorac. Cardiovasc. Surg.* **2003**, *125* (5), 1132–1142.
- (28) Ueda, H.; Nakajima, H.; Hori, Y.; Fujita, T.; Nishimura, M.; Goto, T.; Okuhara, M. Fr901228, A novel antitumor bicyclic depsipeptide produced by *Chromobacterium violaceum*, No-968. 1. Taxonomy, fermentation, isolation, physicochemical and biological properties, and antitumor activity. *J. Antibiot.* **1994**, *47* (3), 301–310.
- (29) Ueda, H.; Manda, T.; Matsumoto, S.; Mukumoto, S.; Nishigaki, F.; Kawamura, I.; Shimomura, K. Fr901228, A novel, antitumor, Bicyclic, Depsipeptide, Produced, by *Chromobacterium violaceum*, No-968. 3. Antitumor activities on experimental tumors in mice. *J. Antibiot.* **1994**, *47* (3), 315–323.
- (30) Ohya, Y.; Toyohara, M.; Sasakawa, M.; Arimura, H.; Ouchi, T. Thermosensitive biodegradable polydepsipeptide. *Macromol. Biosci.* **2005**, *5* (4), 273–276.
- (31) Ouchi, T.; Nozaki, T.; Okamoto, Y.; Shiratani, M.; Ohya, Y. Synthesis and enzymatic hydrolysis of polydepsipeptides with functionalized pendant groups. *Macromol. Chem. Phys.* **1996**, *197* (6), 1823–1833.
- (32) Ouchi, T.; Miyazaki, H.; Arimura, H.; Tasaka, F.; Hamada, A.; Ohya, Y. Synthesis of biodegradable amphiphilic AB-type diblock copolymers of lactide and depsipeptide with pendant reactive groups. *J. Polym. Sci., Part A: Polym. Chem.* **2002**, *40* (9), 1218–1225.
- (33) Tasaka, F.; Ohya, Y.; Ouchi, T. Synthesis of novel comb-type polylactide and its biodegradability. *Macromolecules* **2001**, *34* (16), 5494–5500.
- (34) Ohya, Y.; Matsunami, H.; Yamabe, E.; Ouchi, T. Cell attachment and growth on films prepared from poly(depsipeptide-co-lactide) having various functional groups. *J. Biomed. Mater. Res., Part A* **2003**, *65* (1), 79–88.
- (35) Daura, X.; Jaun, B.; Seebach, D.; van Gunsteren, W. F.; Mark, A. E. Reversible peptide folding in solution by molecular dynamics simulation. *J. Mol. Biol.* **1998**, *280* (5), 925–932.
- (36) Daura, X.; van Gunsteren, W. F.; Rigo, D.; Jaun, B.; Seebach, D. Studying the stability of a helical  $\beta$ -heptapeptide by molecular dynamics simulations. *Chemistry—Eur. J.* **1997**, *3* (9), 1410–1417.
- (37) Garcia, A. E.; Sanbonmatsu, K. Y.  $\alpha$ -Helical stabilization by side chain shielding of backbone hydrogen bonds. *Proc. Natl. Acad. Sci. U.S.A.* **2002**, *99* (5), 2782–2787.
- (38) Simmerling, C.; Strockbine, B.; Roitberg, A. E. All-atom structure prediction and folding simulations of a stable protein. *J. Am. Chem. Soc.* **2002**, *124* (38), 11258–11259.
- (39) Frisch, M. J.; Trucks, G. W.; Schlegel, H. B.; Scuseria, G. E.; Robb, M. A.; Cheeseman, J. R.; Montgomery, J. A., Jr.; Vreven, T.; Kudin, K. N.; Burant, J. C.; Millam, J. M.; Iyengar, S. S.; Tomasi, J.; Barone, V.; Mennucci, B.; Cossi, M.; Scalmani, G.; Rega, N.; Petersson, G. A.; Nakatsuji, H.; Hada, M.; Ehara, M.; Toyota, K.; Fukuda, R.; Hasegawa, J.; Ishida, M.; Nakajima, T.; Honda, Y.; Kitao, O.; Nakai, H.; Klene, M.; Li, X.; Knox, J. E.; Hratchian, H. P.; Cross, J. B.; Bakken, V.; Adamo, C.; Jaramillo, J.; Gomperts, R.; Stratmann, R. E.; Yazyev, O.; Austin, A. J.; Cammi, R.; Pomelli, C.; Ochterski, J. W.; Ayala, P. Y.; Morokuma, K.; Voth, G. A.; Salvador, P.; Dannenberg, J. J.; Zakrzewski, V. G.; Dapprich, S.; Daniels, A. D.; Strain, M. C.; Farkas, O.; Malick, D. K.; Rabuck, A. D.; Raghavachari, K.; Foresman, J. B.; Ortiz, J. V.; Cui, Q.; Baboul, A. G.; Clifford, S.; Cioslowski, J.; Stefanov, B. B.; Liu, G.; Liashenko, A.; Piskorz, P.; Komaromi, I.; Martin, R. L.; Fox, D. J.; Keith, T.; Al-Laham, M. A.; Peng, C. Y.; Nanayakkara, A.; Challacombe, M.; Gill, P. M. W.; Johnson, B.; Chen, W.; Wong, M. W.; Gonzalez, C.; Pople, J. A. *Gaussian 03*; Gaussian, Inc.: Wallingford, CT, 2004.
- (40) Miertus, S.; Scrocco, E.; Tomasi, J. Electrostatic interaction of a solute with a continuum. A direct utilization of ab initio molecular potentials for the prevision of solvent effects. *Chem. Phys.* **1981**, *55* (1), 117–129.
- (41) Jorgensen, W. L.; Maxwell, D. S.; TiradoRives, J. Development and testing of the OPLS all-atom force field on conformational energetics and properties of organic liquids. *J. Am. Chem. Soc.* **1996**, *118* (45), 11225–11236.
- (42) Jorgensen, W. L.; Tirado-Rives, J. Potential energy functions for atomic-level simulations of water and organic and biomolecular systems. *Proc. Natl. Acad. Sci. U.S.A.* **2005**, *102* (19), 6665–6670.

- (43) Breneman, C. M.; Wiberg, K. B. Determining atom-centered monopoles from molecular electrostatic potentials. The need for high sampling density in formamide conformational analysis. *J. Comput. Chem.* **1990**, *11* (3), 361–373.
- (44) Berendsen, H. J. C.; van der Spoel, D.; van Drunen, R. GRO-MACS: A message-passing parallel molecular dynamics implementation. *Comput. Phys. Commun.* **1995**, *91* (1–3), 43–56.
- (45) Lindahl, E.; Hess, B.; van der Spoel, D. GROMACS 3.0: A package for molecular simulation and trajectory analysis. *J. Mol. Model.* **2001**, *7* (8), 306–317.
- (46) Berendsen, H. J. C.; Postma, J. P. M.; van Gunsteren, W. F.; Hermans, J. Interaction models for water in relation to protein hydration. In *Intermolecular Forces*; Pullman, B., Ed.; D. Reidel Publishing: Dordrecht, 1981, pp 331–342.
- (47) Hess, B.; Bekker, H.; Berendsen, H. J. C.; Fraaije, J. G. E. M. LINCS: A linear constraint solver for molecular simulations. *J. Comput. Chem.* **1997**, *18* (12), 1463–1472.
- (48) Nosé, S. A molecular dynamics method for simulations in the canonical ensemble. *Mol. Phys.* **1984**, *52* (2), 255–268.
- (49) Hoover, W. G. Canonical dynamics: Equilibrium phase-space distributions. *Phys. Rev. A* **1985**, *31* (3), 1695–1697.
- (50) Darden, T.; York, D.; Pedersen, L. Particle mesh Ewald—An  $N$ -log- $N$  method for Ewald sums in large systems. *J. Chem. Phys.* **1993**, *98* (12), 10089–10092.
- (51) Essmann, U.; Perera, L.; Berkowitz, M. L.; Darden, T.; Lee, H.; Pedersen, L. G. A smooth particle mesh Ewald method. *J. Chem. Phys.* **1995**, *103* (19), 8577–8593.
- (52) Sugita, Y.; Okamoto, Y. Replica-exchange molecular dynamics method for protein folding. *Chem. Phys. Lett.* **1999**, *314* (1–2), 141–151.
- (53) Yoda, T.; Sugita, Y.; Okamoto, Y. Comparisons of force fields for proteins by generalized-ensemble simulations. *Chem. Phys. Lett.* **2004**, *386* (4–6), 460–467.
- (54) Zhou, R. H. Trp-cage: Folding free energy landscape in explicit water. *Proc. Natl. Acad. Sci. U.S.A.* **2003**, *100* (23), 13280–13285.
- (55) Ferrenberg, A. M.; Swendsen, R. H. Optimized Monte Carlo data analysis. *Phys. Rev. Lett.* **1989**, *63* (12), 1195–1198.
- (56) Garcia, A. E.; Sanbonmatsu, K. Y. Exploring the energy landscape of a  $\beta$  hairpin in explicit solvent. *Proteins: Struct., Funct., Genet.* **2001**, *42* (3), 345–354.
- (57) Wang, X. L.; Vitalis, A.; Wyczalkowski, M. A.; Pappu, R. V. Characterizing the conformational ensemble of monomeric polyglutamine. *Proteins: Struct., Funct., Bioinf.* **2006**, *63* (2), 297–311.
- (58) Gallicchio, E.; Andrec, M.; Felts, A. K.; Levy, R. M. Temperature weighted histogram analysis method, replica exchange, and transition paths. *J. Phys. Chem. B* **2005**, *109* (14), 6722–6731.
- (59) Ramachandran, G. N.; Ramakrishnan, C.; Sasisekharan, V. Stereochemistry of polypeptide chain configurations. *Curr. Sci.* **1990**, *59* (17–18), 813–817.
- (60) Han, W. G.; Elstner, M.; Jalkanen, K. J.; Frauenheim, T.; Suhai, S. Hybrid SCC-DFTB/molecular mechanical studies of H-bonded systems and of  $N$ -acetyl-(L-Ala) $_n$   $N'$ -methylamide helices in water solution. *Int. J. Quantum Chem.* **2000**, *78* (6), 459–479.
- (61) Hovmöller, S.; Zhou, T.; Ohlson, T. Conformations of amino acids in proteins. *Acta Crystallogr., Sect. D: Biol. Crystallogr.* **2002**, *58*, 768–776.
- (62) Donnini, S.; Mark, A. E.; Juffer, A. H.; Villa, A. Incorporating the effect of ionic strength in free energy calculations using explicit ions. *J. Comput. Chem.* **2005**, *26* (2), 115–122.
- (63) Creamer, T. P. Left-handed polyproline II helix formation is (very) locally driven. *Proteins: Struct., Funct., Genet.* **1998**, *33* (2), 218–226.
- (64) Krimm, S.; Mark, J. E. Conformations of polypeptides with ionized side chains with equal length. *Proc. Natl. Acad. Sci. U.S.A.* **1968**, *60*, (44), 1122–1129.
- (65) Hopfinger, A. J. *Intermolecular Interactions and Biomolecular Organization*; John Wiley & Sons: New York, 1977; p 260.
- (66) Jha, A. K.; Colubri, A.; Zaman, M. H.; Koide, S.; Sosnick, T. R.; Freed, K. F. Helix, sheet, and polyproline II frequencies and strong nearest neighbor effects in a restricted coil library. *Biochemistry* **2005**, *44* (28), 9691–9702.
- (67) Mezei, M.; Fleming, P. J.; Srinivasan, R.; Rose, G. D. Polyproline II helix is the preferred conformation for unfolded polyaniline in water. *Proteins: Struct., Funct., Bioinf.* **2004**, *55* (3), 502–507.
- (68) Mezei, M.; Srinivasan, R.; Fleming, P. J.; Rose, G. D. Solvent effect on the conformational preference of poly alanine. *Biophys. J.* **2004**, *86* (1), 630A.
- (69) The gyration tensor is a tensor that describes the second moments of position of a collection of atoms or particles using the formula:  $T_{mn} = (1/(N + 1)) \sum_{i=0}^N r_m^{(i)} r_n^{(i)}$  where  $r_m^{(i)} = s_m^{(i)} - s_{cm}$ ,  $s_m^{(i)}$  is the  $m$ th coordinate of the position vector of the  $i$ th atom, and  $s_{cm}$  is the position vector of the center of mass.

BM070244C